Research Square

Preprints are preliminary reports that have not undergone peer review.
They should not be considered conclusive, used to inform clinical practice,
or referenced by the media as validated information.

Enhancing flame retardancy of PLA with cellulose additives – effects of cellulose content and particle size

Bettina Ötvös
Budapest University of Technology and Economics
Kata Enikő Decsov
Budapest University of Technology and Economics
Szabina Kissová
Budapest University of Technology and Economics
Dániel Gere
Budapest University of Technology and Economics
Katalin Bocz
bocz.katalin@vbk.bme.hu
Budapest University of Technology and Economics

Research Article

Keywords: cellulose microfibre, poly(lactic acid), flame retardancy, thermal properties, mechanical properties, biocomposite

Posted Date: September 3rd, 2026

DOI: https://doi.org/10.21203/rs.3.rs-10381835/v1

License: This work is licensed under a Creative Commons Attribution 4.0 International License.
Read Full License

Additional Declarations: No competing interests reported.

Abstract

The influence of cellulose fibre content and fibre length on the thermal, mechanical, and flame-retardant properties of poly(lactic acid) (PLA) composites containing 15 wt% ammonium polyphosphate (APP) was investigated. Composites containing 5 and 10 wt% cellulose fibres of different lengths were characterised by thermogravimetric analysis (TGA), differential scanning calorimetry (DSC), limiting oxygen index (LOI), UL 94 burning test, cone calorimetry, flexural testing, and compression testing of the combustion residues. Cellulose incorporation slightly reduced the initial thermal stability of the composites but increased char residue, indicating enhanced char-forming capability. DSC analysis showed that cellulose fibres significantly influenced the crystallisation behaviour of PLA; short fibres at 5 wt% provided the most effective nucleating effect. All cellulose-containing formulations achieved a UL 94 V-0 classification, demonstrating the synergistic flame-retardant effect of APP and cellulose fibres. Among the investigated composites, the formulation containing 5 wt% long (60 μm) cellulose fibres reached the highest LOI, the lowest peak heat release rate and total smoke production, which was associated with the greatest expansion of the intumescent char. Compression testing confirmed that this formulation also produced the mechanically most stable combustion residue, establishing a clear correlation between char integrity and improved fire performance. This mechanically reinforced char effectively reduced both heat release and smoke generation, demonstrating that optimizing cellulose fibre geometry and concentration is essential for developing sustainable PLA composites with enhanced flame retardancy, smoke suppression, and mechanical performance.

1 Introduction

Poly(lactic acid) (PLA) has emerged as one of the most widely studied bio-based thermoplastics due to its renewable origin, compostability, and good processability, but its intrinsic flammability and melt dripping behaviour critically limit its use in applications with stringent fire safety requirements. To overcome these drawbacks, intumescent and condensed-phase flame retardant strategies–particularly systems based on phosphorus-containing additives–have attracted sustained attention, as they can promote char formation while preserving the overall ecofriendly character of the material [1].

Among phosphorus-containing flame retardants, ammonium polyphosphate (APP) is one of the most effective and industrially relevant additives for PLA because it can promote the formation of an intumescent, thermally stable char layer through acid-catalysed dehydration, thereby inhibiting heat transfer, oxygen diffusion, and volatile release, leading to reduced peak heat release rate, improved limiting oxygen index (LOI) and, in optimized formulations, UL 94 V-0 ratings. However, high APP loadings, often required to reach demanding fire performance criteria, tend to deteriorate mechanical properties and transparency, and can compromise processability. This has motivated research into synergistic co-additives and architectures that maximise condensed-phase protection at lower total filler loadings [2]. Bio-derived charring agents such as lignin [3], starch [4] or cellulosic fibres [5] have therefore been widely explored as carbon sources in intumescent PLA systems, enabling more sustainable

formulations and, in several cases, providing simultaneous improvements in toughness or stiffness [1, 6–8].

Cellulose is particularly attractive in this context because its dehydration and aromatization under fire conditions promote char formation, and its fibrous morphology can contribute to mechanical reinforcement and barrier effects. Numerous studies have demonstrated that cellulose micro- and nanofibres, when combined with APP can significantly lower the peak heat release rate of PLA, increase char yield, and, in optimized systems, yield UL 94 V-0 ratings at relatively low total additive content [1, 9, 10]. At the same time, the mechanical performance of PLA-cellulose composites is strongly influenced by fibre dimensions, dispersion, and interfacial adhesion [11, 12]. In particular, short or nanoscale fibres can enhance stiffness and strength while maintaining ductility, whereas longer microfibres or wood-like fibres at higher loadings can introduce anisotropy, stress concentrations, and processing challenges [13]. Notably, these parameters–fibre dimensions, dispersion, and interfacial interactions–have also been shown to significantly influence the fire performance of such systems [10, 14, 15]. In our previous study [16], PLA composites containing melamine polyphosphate (MPP) as a flame retardant were investigated, and the proportion as well as the length of cellulose fibres were identified as key parameters influencing the performance of the intumescent system. It was determined that fibres with lengths in the range of 30–60 μm provided the most effective fire-retardant behaviour. These fibres were found to show only a moderate candlewick effect, while during combustion, the structural integrity of the fire protective carbonaceous char layer was effectively enhanced.

The beneficial APP-natural fibre interactions have been demonstrated in various PLA systems, including injection moldings [9], multi-layered natural fabric reinforced composites [17], and composite foams [18]. Despite extensive work on APP–cellulose intumescent PLA systems, the specific role of cellulose fibre length on the balance between flame retardancy, char morphology and mechanical response remains only partially understood, as most studies either focus on one cellulose scale (nanofibres, microcrystalline cellulose or wood fibres) or on chemically modified cellulosic fibres [19–22] rather than systematically comparing different fibre lengths in otherwise similar formulations.

The biodegradation of PLA/cellulose composites has been widely investigated, with numerous studies demonstrating that the incorporation of microsized cellulose generally enhances the biodegradability of PLA by increasing its susceptibility to microbial attack [23–25]. However, recent research on the biodegradability, compostability, and ecotoxicity of PLA/cellulose biocomposites has highlighted that degradation behaviour is governed not only by material composition but also by factors such as physical structure, morphology, and fibre distribution within the matrix [26]. In contrast, the influence of commonly used flame retardants (FRs) on the biodegradation of PLA-based systems remains largely unexplored. Recent findings reported by Decsov et al. [27] indicate that APP does not significantly accelerate the initial stages of PLA degradation during composting and may partially leach from the material at an early stage of the process. However, the available data remain limited, and further research is required to better understand the degradation behaviour of cellulose fibre-reinforced PLA composites containing flame retardants.

In this study, we address this gap by formulating PLA/APP bio-composites containing cellulose fibres of two distinct average lengths (8 µm and 60 µm), introduced at 5 and 10 wt% loading, and by additionally preparing hybrid systems in which short and long cellulose fibres are combined in equal proportions at both total loadings. These compositions are used to elucidate how cellulose fibre length and its distribution govern fire performance, char structure and mechanical behaviour in APP-flame-retarded PLA, with the aim of identifying morphology–property relationships that can guide the design of high-performance, bio-based flame-retardant PLA materials. Moreover, the degradation behaviour of the manufactured PLA/APP/cellulose composites under industrial composting conditions is also investigated.

2 Methods and materials

2.1 Materials

Poly(lactic acid) (PLA) composite formulations were prepared using Ingeo™ Biopolymer 3052D (NatureWorks LLC, USA). The formulations included additives such as 0.25% chain extender (Joncryl ADR-4468, BASF SE, Germany) and 1.5% bentonite-type montmorillonite (CLOISITE® 116, BYK Additives, Germany). The flame retardant used was ammonium polyphosphate (APP, Exolit® AP422), which was supplied by Clariant GmbH (Switzerland). The two types of cellulose materials were purchased from JRS PHARMA GmbH & Co. KG. ARBOCEL® UFC 100 is a microcrystalline, ultra-fine, highly pure cellulose powder with a particle size of ~ 8 µm. ARBOCEL® B 600 are highly pure cellulose microfibres. Its average fibre length is around 60 µm (J. RETTENMAIER & SÖHNE GmbH, Germany). Hereinafter, ARBOCEL® UFC 100 is referred to as “short” and ARBOCEL® B 600 is referred to as “long” in the name of the composites. Compositions containing both types of cellulose in equal ratio were named “mix”.

Also, a reference sample was prepared: PLA extruded with APP and co-additives, (PLA/APP_ref). The PLA/APP_ref sample enabled the assessment of cellulose effects in the presence of co-additives by clarifying interactions within flame-retarded PLA composites. The detailed sample compositions are summarized in Table 1.

Table 1
Compositions of the tested flame retarded PLA composites

	FR	UFC100	B 600
	[%]	[%]	[%]
PLA/APP_ref	15.0	0.0	0.0
PLA/APP/C5short	15.0	5.0	0.0
PLA/APP/C5mix	15.0	2.5	2.5
PLA/APP/C5long	15.0	0.0	5.0
PLA/APP/C10short	15.0	10.0	0.0
PLA/APP/C10mix	15.0	5.0	5.0
PLA/APP/C10long	15.0	0.0	10.0

2.2 Sample Preparation

2.2.1 Extrusion

Prior to processing, PLA and the flame-retardant additives were dried at 80°C for 4 hours to remove moisture. Compounding was performed using a twin-screw extruder (LTE 26–44, Labtech Engineering, Thailand), featuring a 26 mm screw diameter and a length-to-diameter ratio of 44:1. The temperature was carefully controlled along the barrel, starting at 160°C up to 180°C, with a screw speed of 80 rpm. The PLA and additives were thoroughly pre-mixed to ensure homogeneous dispersion before feeding into the extruder. The extrudate was pelletized using a strand pelletizer (LZ-120/VS, Labtech Engineering).

2.2.2 Compression Moulding

The pellets were compression moulded into sheets at 180°C under 100 bar pressure using a hydraulic press (P 200 E, COLLIN Lab GmbH, Germany). Samples for flame retardancy tests were prepared as 130 × 130 × 3 mm^3 sheets. For composting tests, smaller specimens were moulded in 120 × 120 × 0.5 mm^3 steel moulds. The sheets were cut to specific dimensions as per testing requirements.

2.3 Testing Methods

2.3.1 Thermogravimetric Analysis (TGA)

Thermal stability was evaluated on a Q5000 TGA system (TA Instruments, USA) under nitrogen flow at 25 mL/min. Samples (~µmg) were heated from 50 to 600°C at a rate of 10°C/min.

2.3.2 Differential Scanning Calorimetry (DSC)

Thermal transitions were measured using a DSC 3 + instrument (Mettler Toledo, Switzerland) with approximately 10 mg samples in open 100 µm aluminium crucibles in nitrogen atmosphere. The thermal cycle involved heating from 25°C to 200°C at 10°C/min, cooling to 25°C at 2°C/min, and a second heating to 200°C at 10°C/min. Data analysis included determination of glass transition, melting temperatures, and degree of crystallinity, accounting for melting and cold crystallization enthalpies, theoretical melting enthalpy of fully crystalline PLA, and additive content.

2.3.3 Flammability Testing

Limiting Oxygen Index (LOI) tests followed ASTM D2863 and were conducted using an FTT0077 apparatus (Fire Testing Technology, UK). Specimens measured 100 mm × 10 mm × 3 mm. UL 94 horizontal and vertical burning tests were performed according to ASTM D635 and D3801 standards. Cone calorimeter (CC) tests used a TCC 918 (Netzsch, Germany) type apparatus and were performed in agreement with the ISO 5660-1 standard. The heat flux was fixed at 35 kW/m^2 during the measurement of the 100 × 100 × 3 mm^3 samples.

2.3.4 Scanning electron microscopy (SEM)

A 6380LVa (JEOL, Tokyo, Japan) type equipment was used at 10 keV accelerating voltage to examine the microstructure of the carbonaceous residues obtained from the cone calorimetry measurements. Before examination, the samples were fixed on the sample holders with conductive double-sided carbon adhesive tape and a JEOL 1200 (JEOL, Tokyo, Japan) ion sputter was used to form a conductive gold layer at the surface of the samples.

2.3.5 Char compression test

To evaluate the mechanical resistance of the carbonaceous residue of the composites after the combustion, char compression tests were carried out according to a previously described method [15]. 40×40×3 mm^3 specimens were burned under 35 kW/m^2 constant heat flux for 5 minutes in a cone calorimeter equipment supplied by Fire Testing Technology Ltd. (East Grinstead, West Sussex, UK). The char samples obtained after the combustion were compressed with constant 30 µm/s speed between two 25 mm diameter metal plates in an Advanced Rheometer AR 2000 (TA Instruments, New Castle, DE, USA) apparatus. According to the method described in previous studies the lower plate was fixed during the measurement.

2.3.6 Dynamic mechanical analysis (DMA)

For the dynamic mechanical analysis (DMA), a DMA Q800 (TA Instruments Inc., USA) was used. The measurements were conducted in dual cantilever mode, and the applied span length was 35 mm. The specimens' width and length were approximately 10 mm × 60 mm. The temperature range was 25–150°C; the heating rate was 2°C/min while applying a deformation of 0.02% and a frequency of 1 Hz.

2.3.7 Three-point bending test

A Zwick Z005 universal testing machine apparatus was used for the comparative static three-point bending tests. For each composition, 5 pieces of 80 × 10 × 3 mm^3 rectangular shaped samples were measured with 64 mm span length and 5 mm/min crosshead speed till the specimen either reached 10% deformation or broke.

2.3.8 Compostability test

Composting studies adhered to the ISO 20200:2023 standard. Samples were buried about 1 cm deep in compost media in polypropylene boxes (300 × 200 × 100 mm^3), equipped with ventilation holes, maintained at 58°C in a ventilated drying cabinet (DN-63, Baxter International, USA). Specimens (25 × 25 mm^2) were periodically removed over 4 weeks for photographic documentation.

3 Results

3.1 Thermal behaviour and crystallisation properties

3.1.1 TGA analysis

Table 2
TGA results of PLA/APP/cellulose composites

	T_{onset}	T_{max}	V_{max}	Residue @600°C
	[°C]	[°C]	[%/°C]	[%]
PLA/APP_ref	335.1	361.7	2.3	12.6
PLA/APP/C5short	329.4	355.3	2.1	15.9
PLA/APP/C5mix	330.0	357.6	2.0	15.6
PLA/APP/C5long	329.7	358.3	2.0	15.2
PLA/APP/C10short	330.7	355.6	2.1	18.7
PLA/APP/C10mix	326.9	352.4	2.0	19.8
PLA/APP/C10long	326.9	356.5	1.8	16.8

The thermogravimetric analysis (TGA) results provide insight into the thermal stability and decomposition behaviour of PLA/APP composites containing cellulose fibres at different loadings (5 wt% and 10 wt%) and morphologies (short, mixed, and long). The obtained TGA results are summarised in Table 2. The neat PLA/APP_ref sample has an onset degradation temperature (T_{onset}) of 335.1°C and a maximum degradation temperature (T_{max}) of 361.7°C, indicating the highest thermal stability among all investigated systems. This suggests that the addition of cellulose fibres generally introduces an earlier onset of thermal degradation, likely due to the lower thermal stability of cellulose compared to PLA [9]. Across all cellulose-containing formulations, the lowest T_{onset} is observed in the C10mix and

C10long systems (T_{onset} = 326.9°C), indicating that higher cellulose content combined with less favourable fibre morphology accelerates the initial thermal decomposition. A similar trend is observed for T_{max}, which shifts from 361.7°C for the reference sample to lower values in cellulose-containing systems (approximately 352–358°C). The reduction in T_{max} suggests that the presence of cellulose fibres slightly facilitates the overall decomposition process of the PLA matrix, possibly by promoting heat and mass transfer within the composite and altering degradation pathways at the interface. The maximum degradation rate (V_{max}) values show, however, an opposite trend. Lower V_{max} values correspond to the cellulose containing composites, which reflects more gradual degradation behaviour, likely associated with more complex char formation pathways in the presence of cellulose fibres. This assumption is further supported by the residual mass data. Namely, the residual mass at 600°C increases from 12.6% for the PLA/APP_ref sample to values between 15.2% and 19.8% for the cellulose-containing composites. This enhancement in char residue is attributed to the intrinsic char-forming ability of cellulose, which contributes to the formation of a more stable carbonaceous structure during thermal degradation [16].

The incorporation of cellulose generally leads to higher char yields compared to the reference system, although the magnitude of this increase was influenced by fibre morphology in addition to cellulose content. Among the different morphologies, the mixed-fibre systems generally had the highest residual masses at both 5 wt% and 10 wt% cellulose loadings. This suggests that a combination of fibre lengths may promote more effective char network formation, possibly due to improved packing efficiency and more heterogeneous nucleation of the carbonaceous phase. The increased char yield is generally beneficial from a flame-retardancy perspective, as it indicates enhanced condensed-phase barrier formation, which can slow down heat and mass transfer during combustion.

3.1.2 DSC

Table 3
DSC results of PLA/APP/cellulose composites

	T_{m1}*	X_1*	T_c	T_{g2}**	T_{m2}**	X_2**
	[°C]	[%]	[°C]	[°C]	[°C]	[%]
PLA/APP_ref	144.9	1.8	-	59.7	144.8	5.2
PLA/APP/C5short	144.2	3.4	107.7	60.9	142.9	19.0
PLA/APP/C5mix	143.6	2.4	97.1	60.5	143.4	12.1
PLA/APP/C5long	144.3	2.6	95.4	60.5	144.2	8.9
PLA/APP/C10short	143.8	3.0	98.6	60.6	143.9	8.7
PLA/APP/C10mix	144.5	1.1	-	60.7	144.1	8.5
PLA/APP/C10long	144.2	0.3	-	60.9	144.5	3.8
*determenied from the first heating cycle						
**determenied from the second heating cycle						

The DSC results shown in Table 3 demonstrate that the incorporation of ammonium polyphosphate (APP) and cellulose fibres has a limited effect on the thermal transition temperatures of PLA, while noticeably influencing its crystallisation behaviour. The glass transition temperature (T_{g2}) remains essentially constant across all formulations (59.7–60.9°C), indicating that neither APP nor cellulose fibres substantially affect the segmental mobility of the PLA amorphous phase. Similarly, the melting temperatures (T_{m1} and T_{m2}) remain in the range of approximately 143–145°C, indicating that neither cellulose content nor fibre morphology alters the crystalline phase stability of PLA.

A more pronounced effect of cellulose addition is observed in the crystallisation behaviour during cooling (T_c). In the cooling scan of the neat PLA/APP_ref sample does not appear a detectable crystallisation peak, indicating very slow crystallisation kinetics under the applied cooling conditions. In contrast, most cellulose-containing systems show well-defined crystallisation peaks between approximately 95 and 108°C, confirming that cellulose can act as a heterogeneous nucleating agent for PLA [12, 28]. The extent of this nucleating effect is strongly dependent on fibre morphology and loading. The highest crystallisation temperature (T_c = 107.7°C) is observed for the PLA/APP/C5short system, indicating the most rapid crystallisation and the most efficient nucleation. This behaviour can be attributed to the high specific surface area and more homogeneous dispersion of short fibres, which provide a larger number of effective nucleation sites for PLA crystal formation. In comparison, systems containing mixed and long fibres have lower T_c values (approximately 95–99°C), suggesting slower crystallisation kinetics. The reduced nucleation efficiency in these systems is likely related to decreased effective surface area per unit mass, fibre entanglement, and less uniform dispersion, which collectively

limit polymer–fibre interfacial interactions. An increase in cellulose content from 5 wt% to 10 wt% does not further enhance crystallisation behaviour. In fact, PLA/APP/C10mix and PLA/APP/C10long systems do not show a clearly defined crystallisation peak, indicating strongly hindered or suppressed crystallisation under the applied cooling conditions. This suggests that at higher filler loading, fibre aggregation and restricted chain mobility become dominant effects, outweighing any potential increase in nucleation site density. In this respect, an optimal filler content appears to exist around 5 wt%, where nucleation is maximised without significantly restricting PLA chain mobility. The degree of crystallinity, evaluated from the first (X_1) and second (X_2) heating runs, further supports these observations. The first heating scan reflects the as-processed morphology, while the second heating scan provides insight into the material's ability to reorganise after thermal history removal. The neat PLA/APP_ref sample has very low crystallinity (X_1 = 1.8%, X_2 = 5.2%), confirming its predominantly amorphous nature. The addition of cellulose leads to a noticeable increase in crystallinity, particularly for the C5short system, which reaches the highest crystallinity values (X_1 = 3.4%, X_2 = 19.0%). Systems with higher cellulose loading and longer fibres tend to exhibit reduced crystallinity, consistent with restricted polymer chain mobility and less efficient crystal growth.

3.2 Flame retardancy behaviour

3.2.1 LOI and UL 94

The flammability properties of PLA-based composites were significantly improved by the incorporation of ammonium polyphosphate (APP) and cellulose fibres, as demonstrated by limiting oxygen index values and UL 94 test results presented in Fig. 1. The reference PLA sample (PLA_ref) had a low LOI value of 20.0% and was classified as HB, with a horizontal burning rate of 23.7 mm/min, confirming its inherent high flammability. The addition of 15 wt% APP (PLA/APP_ref) increased the LOI to 33.0% and improved the UL 94 classification to V-2, indicating enhanced flame retardancy. The incorporation of cellulose fibres (5 or 10 wt%) into the PLA/APP system led to further improvements, with all fibre-containing composites achieving a V-0 classification, indicating self-extinguishing behaviour without dripping. However, clear differences were observed in LOI values as a function of fibre loading and fibre type.

At 5 wt% fibre content, LOI values ranged from 38.5% to 40.0%, with long fibres (PLA/APP/C5long) providing the highest value. Mixed and short fibres resulted in slightly lower LOI values (39.5% and 38.5%, respectively). Increasing the fibre content to 10 wt% generally led to a reduction in LOI (35.0–38.0%), although all samples maintained V-0 classification. Within this group, long fibres (PLA/APP/C10long) again showed the best performance, while short and mixed fibres showed comparatively lower LOI values. These results suggest that cellulose fibres act synergistically with APP to enhance char formation and improve flame retardancy. Fibre length appears to play a role, with longer fibres generally contributing to higher LOI values, possibly due to improved structural integrity and stability of the protective char layer. However, increasing fibre content from 5% to 10% does not lead to

further improvement and slightly reduces efficiency, potentially due to agglomeration or disruption of the intumescent char structure.

3.2.2 Cone calorimetry

Table 4
Combustion characteristics of the PLA/APP/cellulose composites

	TTI	Burning time	MARHE	pHRR	THR	TSP	Residue
	[s]	[s]	[kW/m^2]	[kW/m^2]	[MJ/m^2]	[m^2/m^2]	[%]
PLA_ref	85 ± 7	281 ± 12	214 ± 5	353 ± 2	69.9 ± 1.2	12 ± 5	0.3 ± 0.0
PLA/APP_ref	71 ± 0	963 ± 48	61 ± 1	190 ± 3	53.2 ± 1.3	82 ± 10	19.3 ± 1.3
PLA/APP/C5short	69 ± 3	485 ± 18	119 ± 2	214 ± 4	60.5 ± 0.3	167 ± 6	18.3 ± 0.1
PLA/APP/C5mix	70 ± 7	600 ± 18	112 ± 3	202 ± 1	59.9 ± 2.4	93 ± 31	19.1 ± 0.2
PLA/APP/C5long	69 ± 5	743 ± 76	94 ± 4	182 ± 3	55.6 ± 0.2	96 ± 57	19.6 ± 0.1
PLA/APP/C10short	64 ± 3	407 ± 58	134 ± 4	202 ± 7	59.3 ± 1.0	325 ± 6	19.2 ± 0.3
PLA/APP/C10mix	73 ± 12	491 ± 38	117 ± 1	193 ± 6	60.8 ± 2.8	330 ± 12	20.2 ± 0.1
PLA/APP/C10long	62 ± 4	472 ± 25	119 ± 0	194 ± 2	59.6 ± 0.6	228 ± 28	18.5 ± 0.1

The cone calorimeter results, presented in Fig. 2. and Table 4, respectively, further confirm the significant improvement in fire performance of PLA upon incorporation of APP and highlight the additional influence of cellulose fibre content and morphology. The reference PLA sample (PLA_ref) shows typical behaviour of a highly flammable polymer, with a high peak heat release rate (pHRR = 353 kW/m^2), high MARHE (214 kW/m^2), and negligible residue (0.3%), indicating the absence of effective char formation. The addition of APP (PLA/APP_ref) drastically reduces pHRR (by 46%) and MARHE (by 72%), while increasing residue to ~ 19%, confirming the formation of an intumescent protective char, which acts as an effective barrier to heat and mass transfer. The reduction in total heat release (THR) further confirms the enhanced fire resistance of the system, despite a slight decrease in time to ignition (TTI), which is commonly observed in APP-containing formulations due to early onset of decomposition and acid-catalysed dehydration reactions [29, 30].

The introduction of cellulose fibres into the PLA/APP system reveals a more complex behaviour, strongly dependent on fibre content and morphology. At 5 wt% fibre loading, the composites show moderate

increases in pHRR and MARHE compared to PLA/APP_ref, particularly for short and mixed fibres. However, the sample with long fibres (PLA/APP/C5long) reached the lowest pHRR (182 kW/m^2) among the fibre-containing systems and a relatively low MARHE (94 kW/m^2), approaching the performance of PLA/APP_ref. This suggests that long fibres contribute positively to fire performance, likely by reinforcing the intumescent char and improving its structural integrity. At 5 wt% cellulose content, THR values remain relatively low (~ 56–60 MJ/m^2), and residue formation is maintained (~ 18–20%), indicating that the condensed-phase flame retardant mechanism is preserved.

At 10 wt% fibre loading, a general deterioration in fire performance is observed. MARHE increases (up to 134 kW/m^2 for short fibres), and pHRR values remain consistently higher than for the APP-only reference. Additionally, THR slightly increases, and TTI tends to decrease, indicating an overall increase in flammability. A particularly notable effect is the substantial increase in total smoke production (TSP), especially for short and mixed fibres (up to ~ 330 m^2/m^2), which suggests less efficient combustion or more likely disruption of the protective char layer.

These trends can be explained as the result of competing mechanisms. On one hand, cellulose fibres promote char formation and can act as a reinforcing scaffold for the intumescent layer generated by APP. On the other hand, at higher fibre loadings, the structural integrity of the char may be compromised. This can facilitate the transport of molten polymer and volatile degradation products towards the flame zone, thereby sustaining combustion. This adverse effect is likely more pronounced for short fibres due to their lower aspect ratio and reduced ability to form a continuous reinforcing network within the char. Consequently, the char layer becomes more porous and less mechanically coherent, reducing its barrier efficiency. The heat release rate (HRR) curves (Fig. 2) support this interpretation. While the PLA/APP_ref sample has a reduced and broadened HRR curve, the fibre-containing composites – particularly at 10 wt% – show a shorter overall burning duration accompanied by higher pHRR values. The combination of shortened burning time and increased HRR suggests that the protective char layer is less effective in sustaining a stable barrier. Instead of providing prolonged thermal insulation and gradual degradation, the char appears to be more porous and less coherent, which facilitates faster heat feedback and accelerated fuel volatilisation.

In summary, the cone calorimeter results demonstrate that fire performance is governed by a balance between char reinforcement and fibre-induced disruption of the protective layer. The optimal performance is achieved at lower fibre content (5 wt%) and with long fibres, which most effectively support the formation of a cohesive intumescent char while minimising structural degradation effects.

3.3 Analysis of char structure

3.3.1 Photographs of the combustion residues

Photographs of the combustion residues remaining after the cone calorimetry test are presented in Fig. 3. Compared with PLA/APP_ref, all cellulose-containing samples showed lower expansion of the intumescent char layer, except for the composite containing 5 wt% long cellulose fibres, which had a

comparable foam height. This observation suggests that cellulose fibres generally limit the expansion of the intumescent foam. However, at an appropriate fibre size and concentration, the fibres can become incorporated into the carbonaceous structure, acting as a reinforcing framework that stabilizes the char layer and allows foam expansion comparable to that of the reference material. The height and stability of the intumescent char layer are directly related to the heat-shielding performance of the material. The enhanced char expansion and structural stability observed for the PLA/APP/C5long composite contributed to its superior fire-retardant performance, as demonstrated by the cone calorimeter measurements (see Fig. 2 and Table 4).

It can be also observed in Fig. 3 that the residue of PLA/APP_ref is noticeably grayer than those of the cellulose-containing composites, which is likely associated with a higher degree of graphitisation of the char.

3.3.2 SEM analysis of the chars

The microstructures of the char residues obtained after cone calorimetry are shown in Fig. 4, as observed by SEM. It can be seen that both cellulose content and fibre morphology markedly influence the structure of the protective char layer. Formulations containing 5 wt% cellulose generally produced more compact and continuous chars than those containing 10 wt% cellulose. At the lower cellulose loading, the APP/cellulose system appears to promote efficient intumescence, resulting in the formation of an expanded carbonaceous network with good structural integrity. The most effective residue was obtained for the PLA/APP/C5long sample, which showed a well-developed intumescent morphology characterized by an interconnected and continuous structure. The char walls were relatively thick and cohesive, suggesting enhanced mechanical stability and improved resistance to heat and mass transfer during combustion. Such a morphology is consistent with the superior flame-retardant performance observed during cone calorimetry (see Fig. 2). Increasing the cellulose content to 10 wt% resulted in a less homogeneous char structure. Although char formation was still promoted, the residues contained a greater number of defects, larger voids, and regions of structural collapse.

The influence of fibre morphology is particularly evident when comparing long and short cellulose fibres. Long fibres promoted the formation of interconnected char networks that reinforced the intumescent structure and improved residue continuity. In contrast, short fibres generated more fragmented and loosely packed carbonaceous residues. The reduced integrity of these char layers likely reduced their barrier function, explaining the inferior flame-retardant performance of these formulations.

The SEM observations indicate that an optimal balance between cellulose content and fibre morphology is required to maximize the effectiveness of the APP-based flame-retardant system. The combination of 5 wt% long cellulose fibres produced the most robust protective char, whereas increasing the cellulose loading to 10 wt% and reducing the fibre length led to the formation of less effective residues.

3.3.3 Char expansion

Figure 5 compares the height of the combustion residue (char) formed after exposing the PLA/APP/cellulose composites to a constant external heat flux of 35 kW/m^2 for 5 min. The reference PLA/APP_ref sample produced an expanded char with a height of approximately 25.5 mm. The incorporation of 5 wt% short cellulose fibres reduced the char height to 17.9 mm, whereas the composite containing 5 wt% long cellulose fibres (PLA/APP/C5long) produced the highest char height (27.8 mm) of all formulations. The composite containing 5 wt% mixed fibre lengths had an intermediate char height (20.5 mm).

Increasing the cellulose fibre content to 10 wt% resulted in a reduction in char height irrespective of fibre length. Among these composites, the PLA/APP/C10long formulation had the lowest char height (13.3 mm). These results indicate that, at a cellulose loading of 5 wt%, long fibres promoted the expansion of the intumescent char beyond that of the PLA/APP reference, whereas short fibres reduced char expansion. In contrast, increasing the cellulose content to 10 wt% suppressed the expansion of the protective char layer for all fibre lengths, suggesting that excessive cellulose adversely affected the efficiency of the APP-based intumescent system.

The enhanced char expansion observed for the PLA/APP/C5long composite is likely associated with the reinforcing effect of the long cellulose fibres within the intumescent char. During combustion, the long fibres may act as a reinforcing framework, improving the mechanical integrity of the expanding char layer and reducing its tendency to collapse. In contrast, short fibres appear to provide less effective reinforcement and may interrupt the continuity of the expanding char, resulting in lower char heights. At the higher cellulose loading (10 wt%), the reduction in char height suggests that excessive fibre content interfered with the expansion of the APP-based intumescent structure, possibly by increasing melt viscosity, disturbing the optimum APP-to-carbon ratio, or promoting premature collapse of the expanding char.

3.3.4 Char mechanical properties

To further evaluate the structural integrity of the combustion residues, compression tests were performed on the chars (Fig. 6). At low deformations (up to 5%), the residues produced by the PLA/APP/C5mix and PLA/APP/C5long composites showed the highest compressive forces, indicating the formation of mechanically robust intumescent chars. In contrast, the chars produced by the composites containing 10 wt% cellulose fibres exhibited substantially lower compressive forces, indicating weaker and less cohesive char structures.

The superior mechanical stability of the PLA/APP/C5long char is consistent with its outstanding fire performance, as this formulation also reached the highest limiting oxygen index (LOI), the lowest peak heat release rate (pkHRR), and one of the lowest total smoke production (TSP). These findings suggest that the thick and mechanically reinforced intumescent char acted as a more effective thermal and mass-transfer barrier during combustion. Consequently, the enhanced integrity of the char appears to be a key factor responsible for the improved flame-retardant performance of the PLA/APP/C5long composite.

3.4 Mechanical properties

3.4.1 DMA

Table 5
Thermomechanical caracteristics of PLA/APP/cellulose composites

	Storage modulus at 30°C	Max loss modulus	Glass transition temperature*
	[MPa]	[MPa]	[°C]
PLA/APP_ref	3288	738	59.2
PLA/APP/C5short	3459	768	59.2
PLA/APP/C5mix	3303	683	61.0
PLA/APP/C5long	3320	770	60.2
PLA/APP/C10short	3698	811	60.6
PLA/APP/C10mix	3517	730	61.0
PLA/APP/C10long	3409	632	61.2

** Glass transition temperature was defined as the temperature at the maximum point of the loss modulus curve*

The thermomechanical behaviour of the PLA/APP/cellulose composites was evaluated by dynamic mechanical analysis (DMA), and the corresponding storage modulus (E') and tan δ curves are presented in Fig. 7. All formulations showed the typical viscoelastic response of PLA, characterized by a gradual decrease in storage modulus with increasing temperature followed by a sharp drop in the glass transition region between approximately 55 and 65°C. The glass transition was further identified by the presence of a distinct tan δ peak for each sample.

In the glassy region (30–55°C), all cellulose-containing composites had higher storage modulus values than the PLA/APP reference, demonstrating the reinforcing effect of the cellulose fibres. The increased stiffness can be attributed to the high modulus of the cellulose fibres and their ability to bear part of the applied load, thereby reducing deformation of the PLA matrix. The enhancement was particularly evident for composites containing 10 wt% cellulose, which maintained the highest storage modulus values throughout the investigated temperature range.

The incorporation of cellulose also significantly influenced the relaxation behaviour of the PLA matrix. Compared with PLA/APP_ref, all cellulose-containing formulations exhibited lower tan δ peak intensities, indicating reduced damping capability and restricted segmental motion of the polymer chains. Among the cellulose-filled formulations, the long-fibre composites had the lowest tan δ peak intensities, particularly PLA/APP/10long. This behaviour suggests that long fibres are more effective than short

fibres in constraining molecular motion within the PLA matrix. The larger aspect ratio of the long fibres increases the interfacial contact area between the reinforcement and the polymer matrix, resulting in more effective stress transfer and a greater immobilization of polymer chains in the interfacial region. Consequently, a larger fraction of the PLA matrix participates in restricted molecular motion, leading to lower damping behaviour. The broadening of the tan δ peaks observed for some formulations further suggests the existence of heterogeneous relaxation environments within the composites. Such behaviour is commonly associated with the presence of interfacial regions where polymer chain mobility differs from that of the bulk matrix. The combined presence of APP particles and cellulose fibres likely creates a distribution of relaxation times, resulting in broader transitions compared with the reference formulation.

Small variations in the temperature corresponding to the tan δ maximum were also observed (Table 5). The slight shift of the relaxation peak towards higher temperatures for several cellulose-containing composites indicates that greater thermal energy is required to initiate cooperative segmental motion of the PLA chains. This behaviour is consistent with enhanced fibre–matrix interactions and reduced free volume within the composite structure.

Above the glass transition temperature, all samples showed substantial decrease in storage modulus as the PLA matrix entered the rubbery state. However, the cellulose-containing composites retained higher modulus values than PLA/APP_ref, demonstrating that the fibre network continued to provide structural support even after softening of the polymer matrix. The superior modulus retention of the long-fibre systems further highlights the beneficial role of fibre morphology in maintaining mechanical integrity at elevated temperatures.

Overall, the DMA results demonstrate that cellulose fibres improve the thermomechanical performance of PLA/APP composites through both mechanical reinforcement and restriction of molecular mobility. While increasing cellulose content enhances stiffness, fibre morphology plays a crucial role in determining the efficiency of reinforcement. Long fibres were particularly effective in reducing chain mobility, as evidenced by their lower tan δ peak intensities and improved modulus retention. These findings indicate stronger fibre–matrix interactions and more efficient stress transfer in the long-fibre composites, which contribute to their enhanced thermomechanical performance.

3.4.2 Bending test

The flexural properties of the PLA/APP/cellulose composites are presented in Fig. 8. The incorporation of cellulose fibres resulted in a noticeable improvement in flexural stiffness compared with the PLA/APP reference material. The flexural modulus increased from 4025 MPa for PLA/APP_ref to values ranging between 4362 and 4882 MPa for the cellulose-containing composites, corresponding to an increase of approximately 8–21%. This improvement can be attributed to the high intrinsic stiffness of cellulose fibres and their ability to effectively transfer stress within the composite structure.

Among all formulations, the highest flexural modulus (4882 MPa) corresponds to PLA/APP/10small, followed by PLA/APP/10long (4729 MPa) and PLA/APP/10mix (4677 MPa). The higher modulus values observed for the 10 wt% cellulose composites indicate that increasing fibre content enhances the rigidity of the material by increasing the volume fraction of the reinforcing phase. A similar trend was observed in the DMA results, where the cellulose-filled composites had higher storage modulus values than the reference formulation.

Despite the increase in stiffness, the flexural strength was only moderately affected by cellulose incorporation. The flexural strength of PLA/APP_ref was 84.3 MPa, while the composites exhibited values between 82.5 and 88.7 MPa. The highest flexural strength was obtained for PLA/APP/5small (88.7 MPa), representing an increase of approximately 5% compared with the reference material. The remaining formulations showed strength values comparable to the reference, indicating that cellulose addition did not significantly compromise the load-bearing capability of the composites.

The results suggest that the mechanisms controlling flexural modulus and flexural strength differ. While the modulus is primarily governed by the stiffness of the reinforcing fibres, the flexural strength is strongly influenced by fibre dispersion, fibre–matrix adhesion, and the presence of stress-concentrating defects. At higher cellulose loadings (10 wt%), the increased fibre content likely enhanced stiffness but may also have promoted fibre agglomeration or local stress concentrations, limiting further improvements in strength. This effect is particularly evident for PLA/APP/10mix, which exhibited the lowest flexural strength despite possessing a relatively high modulus.

The influence of fibre morphology was less pronounced than the effect of cellulose content. Long fibres generally provided higher modulus values than their 5 wt% counterparts, reflecting their greater aspect ratio and more efficient stress transfer. However, the differences in flexural strength among the short-, mixed-, and long-fibre systems were relatively small and remained within a narrow range.

3.5 Compostability

Figure 9 shows the visual appearance of the PLA/APP/cellulose composites during composting over a period of 28 days. All formulations underwent progressive degradation with increasing composting time, as evidenced by gradual darkening, surface deterioration, loss of structural integrity, and eventual fragmentation. The degradation became more pronounced after approximately 14–16 days of composting and continued throughout the remainder of the test period.

The PLA/APP reference and cellulose-containing composites followed a broadly similar degradation pattern. During the early stages of composting, all specimens largely retained their original shape, while more extensive surface damage and fragmentation became evident at longer exposure times. By day 28, substantial deterioration was observed for all formulations, confirming the susceptibility of the PLA-based composites to degradation under composting conditions.

Although some differences in the extent and morphology of degradation can be observed among the formulations, no clear trend associated with cellulose content or fibre morphology can be conclusively

established from the visual observations alone. Nevertheless, the results demonstrate that the incorporation of cellulose fibres does not hinder the compostability of the PLA/APP system, and all composites underwent significant degradation during the composting period.

4 Conclusion

This study investigated the influence of cellulose fibre content and fibre length on the thermal, mechanical, and flame-retardant properties of PLA composites containing 15 wt% APP.

In general, the incorporation of cellulose fibres slightly reduced the initial thermal stability of the composites, nevertheless, the increased char residue observed by TGA demonstrated an enhanced char-forming capability for all cellulose-containing formulations.

DSC analyses revealed that cellulose fibres significantly affected the crystallisation behaviour of PLA without altering its melting characteristics. Short fibres at 5 wt% acted as the most effective nucleating agents, increasing the crystallisation temperature and degree of crystallinity, whereas longer fibres and higher cellulose loadings reduced crystallisation efficiency because of fibre aggregation and restricted polymer chain mobility. These findings demonstrate that both fibre geometry and concentration are important parameters governing the microstructure of the composites.

The combination of APP and cellulose fibres substantially improved the flame retardancy of PLA, with all fibre-containing formulations achieving a UL 94 V-0 classification. Among the investigated formulations, the composite containing 5 wt% long cellulose fibres (PLA/APP/C5long) showed the best overall fire performance, characterised by the highest LOI, the lowest pHRR and TSP, which was associated with the formation of the most expanded intumescent char layer. Compression testing further demonstrated that this formulation produced the mechanically most stable combustion residue. The correlation between char expansion, char mechanical stability, and the reductions in both pHRR and TSP demonstrates that the integrity of the protective intumescent layer is a key factor governing the fire behaviour and smoke suppression performance of these composites.

In addition to the enhanced flame retardancy, cellulose fibres effectively reinforced the PLA/APP matrix. Increasing cellulose content improved the flexural modulus while maintaining flexural strength, indicating improved resistance to bending without compromising structural performance.

Our results demonstrate that optimizing both cellulose fibre content and fibre length is essential for balancing thermal behaviour, mechanical performance, and flame retardancy in PLA/APP composites. In particular, the incorporation of 5 wt% long (60 μm) cellulose fibres provided the most favourable combination of properties, yielding a mechanically robust intumescent char that effectively reduced heat release and smoke production while maintaining good mechanical performance. These findings highlight the potential of fibre-reinforced intumescent systems for the development of sustainable, high-performance flame-retardant PLA composites with enhanced smoke suppression capabilities.

Declarations

Funding

The research has been implemented with the support provided by the Ministry of Innovation and Technology of Hungary from the National Research, Development and Innovation Fund, financed under the K143039 and PD146135 funding scheme. Bettina Ötvös was supported by the Doctoral Excellence Fellowship Programme (DCEP), funded by the National Research Development and Innovation Fund of the Ministry of Culture and Innovation and the Budapest University of Technology and Economics (DKÖP-25-1-BME-24). Dániel Gere is thankful for the János Bolyai Research Scholarship (BO/00894/ 23/6) of the Hungarian Academy of Sciences.

Competing Interests

The authors declare no competing interest.

Author Contributions

Bettina Ötvös: Writing – original draft, Investigation, Formal analysis, Data curation. **Kata E. Decsov**: Conceptualization, Writing – review & editing, Methodology, Investigation, Formal analysis, Data curation. **Szabina Kissová**: Methodology, Investigation, Formal analysis, Data curation. **Dániel Gere**: Methodology, Investigation, Writing – review & editing. **Katalin Bocz:** Conceptualization, Writing – original draft, Validation, Supervision, Data curation, Conceptualization.

Data availability

Data will be made available on request.

References

1. W. Yin, L. Chen, F. Lu, P. Song, J. Dai, L. Meng, Mechanically robust, flame-retardant poly(lactic acid) biocomposites via combining cellulose nanofibers and ammonium polyphosphate, ACS Omega 3 (2018) 5615–5626. https://doi.org/10.1021/acsomega.8b00540.
2. B. Tawiah, B. Yu, B. Fei, Advances in flame retardant poly(lactic acid), Polymers (Basel). 10 (2018) 876. https://doi.org/10.3390/polym10080876.
3. A. Cayla, F. Rault, S. Giraud, F. Salaün, V. Fierro, A. Celzard, PLA with intumescent system containing lignin and ammonium polyphosphate for flame retardant textile, Polymers (Basel). 8 (2016). https://doi.org/10.3390/polym8090331.
4. M. Maqsood, G. Seide, Investigation of the flammability and thermal stability of halogen-free intumescent system in biopolymer composites containing biobased carbonization agent and mechanism of their char formation, Polymers (Basel). 11 (2019). https://doi.org/10.3390/polym11010048.

5. L. Shumao, R. Jie, Y. Hua, Y. Tao, Y. Weizhong, Influence of ammonium polyphosphate on the flame retardancy and mechanical properties of ramie fiber-reinforced poly(lactic acid) biocomposites, Polym. Int. 59 (2010) 242–248. https://doi.org/10.1002/pi.2715.
6. D.M. Fox, M. Novy, K. Brown, M. Zammarano, R.H. Harris, M. Murariu, E.D. McCarthy, J.E. Seppala, J.W. Gilman, Flame retarded poly(lactic acid) using POSS-modified cellulose. 2. Effects of intumescing flame retardant formulations on polymer degradation and composite physical properties, Polym. Degrad. Stab. 106 (2014) 54–62. https://doi.org/10.1016/j.polymdegradstab.2014.01.007.
7. F. Shukor, A. Hassan, M. Saiful Islam, M. Mokhtar, M. Hasan, Effect of ammonium polyphosphate on flame retardancy, thermal stability and mechanical properties of alkali treated kenaf fiber filled PLA biocomposites, Mater. Des. 54 (2014) 425–429. https://doi.org/10.1016/j.matdes.2013.07.095.
8. W.S. Chow, E.L. Teoh, J. Karger-Kocsis, Flame retarded poly(lactic acid): A review, Express Polym. Lett. 12 (2018) 396–417. https://doi.org/10.3144/expresspolymlett.2018.34.
9. K. Matsumoto, T. Tanaka, M. Sasada, N. Sano, K. Masuyama, A mechanism for fire retardancy realized by a combination of biofillers and ammonium polyphosphate in various polymer systems, Cellulose 28 (2021) 3833–3846. https://doi.org/10.1007/s10570-021-03747-4.
10. Y. Sun, M. Liu, Z. Zhang, H. Liu, D. Shi, J. Ying, W. Mu, D. Li, I. Kong, Effect of silane-modified ammonium polyphosphate on the mechanical, thermal, and flame-retardant properties of rice husk/polylactic acid composites, Journal of Composites Science 9 (2025) 251. https://doi.org/10.3390/jcs9050251.
11. V.C. Agbakoba, T.C. Mokhena, E.E. Ferg, S.P. Hlangothi, M.J. John, PLA bio-nanocomposites reinforced with cellulose nanofibrils (CNFs) for 3D printing applications, Cellulose 30 (2023) 11537–11559. https://doi.org/10.1007/s10570-023-05549-2.
12. T.S. Melo, J.N.S. Almeida, A.B.O.R. Barros, E.S. Medeiros, A.S.F. Santos, Producing well-dispersed cellulose nanocrystals (CNCs) in poly(lactic acid) (PLA), Cellulose (2026). https://doi.org/10.1007/s10570-026-07119-8.
13. A. Awal, M. Rana, M. Sain, Thermorheological and mechanical properties of cellulose reinforced PLA bio-composites, Mechanics of Materials 80 (2015) 87–95. https://doi.org/10.1016/j.mechmat.2014.09.009.
14. M. Kaci, T. Aouat, E. Devaux, J.M. Lopez-Cuesta, The effects of filler size and content on the fire behavior of melt-spun poly(lactic acid)/cellulose bionanocomposite fibers, in: AIP Conf. Proc., American Institute of Physics Inc., 2019. https://doi.org/10.1063/1.5140290.
15. K. Decsov, V. Takács, G. Marosi, K. Bocz, Microfibrous cyclodextrin boosts flame retardancy of poly(lactic acid), Polym. Degrad. Stab. 191 (2021) 109655. https://doi.org/10.1016/j.polymdegradstab.2021.109655.
16. K.E. Decsov, B. Ötvös, T.T.T. Nguyen, K. Bocz, The Effect of cellulose fibre length on the efficiency of an intumescent flame retardant system in poly(lactic acid), Fire 6 (2023) 97. https://doi.org/10.3390/fire6030097.

17. K. Bocz, B. Szolnoki, A. Farkas, E. Verret, D. Vadas, K. Decsov, G. Marosi, Optimal distribution of phosphorus compounds in multi-layered natural fabric reinforced biocomposites, Express Polym. Lett. 14 (2020) 606–618. https://doi.org/10.3144/expresspolymlett.2020.50.
18. D. Vadas, T. Igricz, J. Sarazin, S. Bourbigot, G. Marosi, K. Bocz, Flame retardancy of microcellular poly(lactic acid) foams prepared by supercritical CO2-assisted extrusion, Polym. Degrad. Stab. 153 (2018) 100–108. https://doi.org/10.1016/j.polymdegradstab.2018.04.021.
19. D.M. Fox, S. Temburni, M. Novy, L. Flynn, M. Zammarano, Y.S. Kim, J.W. Gilman, R.D. Davis, Thermal and burning properties of poly(lactic acid) composites using cellulose-based intumescing flame retardants, in: ACS Symposium Series, American Chemical Society, 2012: pp. 223–234. https://doi.org/10.1021/bk-2012-1118.ch016.
20. Y. Guo, S. He, X. Zuo, Y. Xue, Z. Chen, C.C. Chang, E. Weil, M. Rafailovich, Incorporation of cellulose with adsorbed phosphates into poly (lactic acid) for enhanced mechanical and flame retardant properties, Polym. Degrad. Stab. 144 (2017) 24–32. https://doi.org/10.1016/j.polymdegradstab.2017.08.004.
21. L. Costes, F. Laoutid, F. Khelifa, G. Rose, S. Brohez, C. Delvosalle, P. Dubois, Cellulose/phosphorus combinations for sustainable fire retarded polylactide, Eur. Polym. J. 74 (2016) 218–228. https://doi.org/10.1016/j.eurpolymj.2015.11.030.
22. K. Bocz, B. Szolnoki, A. Marosi, T. Tábi, M. Wladyka-Przybylak, G. Marosi, Flax fibre reinforced PLA/TPS biocomposites flame retarded with multifunctional additive system, Polym. Degrad. Stab. 106 (2014) 63–73. https://doi.org/10.1016/j.polymdegradstab.2013.10.025.
23. L.M. Galera Manzano, M.Á. Ruz Cruz, N.M. Moo Tun, A. Valadez González, J.H. Mina Hernandez, Effect of cellulose and cellulose nanocrystal contents on the biodegradation, under composting conditions, of hierarchical PLA biocomposites, Polymers (Basel). 13 (2021) 1855. https://doi.org/10.3390/polym13111855.
24. A. Xu, Y. Wang, J. Gao, J. Wang, Facile fabrication of a homogeneous cellulose/polylactic acid composite film with improved biocompatibility, biodegradability and mechanical properties, Green Chemistry 21 (2019) 4449–4456. https://doi.org/10.1039/C9GC01918A.
25. E. Fortunati, D. Puglia, M. Monti, C. Santulli, M. Maniruzzaman, M.L. Foresti, A. Vazquez, J.M. Kenny, Okra (Abelmoschus esculentus) fibre based PLA composites: Mechanical behaviour and biodegradation, J. Polym. Environ. 21 (2013) 726–737. https://doi.org/10.1007/s10924-013-0571-5.
26. V.L.D. Costa, P.E.M. Videira, A. de O. Mendes, T. Duarte, B.F.A. Valente, P. Pinto, A. Gaspar, T. Viana, P.T. Fiadeiro, J.M.R. Curto, M.E. Amaral, A.P. Costa, J.C. Vieira, Evaluating environmental performance of PLA–Cellulose-based biocomposites: A comprehensive study on biodegradability, compostability, and ecotoxicity, Polymers (Basel). 17 (2025) 3232. https://doi.org/10.3390/polym17233232.
27. K.E. Decsov, B. Ötvös, L. Lengyel, D. Gere, D. Fecske, A. Petróczy, B. Iván, V. Feigl, M. Molnár, K. Bocz, Effects of phosphorus-nitrogen containing flame retardants on the compostability of poly(lactic

acid), Polym. Degrad. Stab. 249 (2026) 112085. https://doi.org/10.1016/j.polymdegradstab.2026.112085.

28. K. Shi, G. Liu, H. Sun, B. Yang, Y. Weng, Effect of biomass as nucleating agents on crystallization behavior of polylactic acid, Polymers (Basel). 14 (2022) 4305. https://doi.org/10.3390/polym14204305.
29. M. Chen, Y. Xu, X. Chen, Y. Ma, W. He, J. Yu, Z. Zhang, Thermal stability and combustion behavior of flame-retardant polypropylene with thermoplastic polyurethane-microencapsulated ammonium polyphosphate, High Perform. Polym. 26 (2014) 445–454. https://doi.org/10.1177/0954008313517910.
30. T. Liu, J. Jing, Y. Zhang, Z. Fang, Synthesis of a novel polyphosphate and its application with APP in flame retardant PLA, RSC Adv. 8 (2018) 4483–4493. https://doi.org/10.1039/C7RA12582H.

Figures

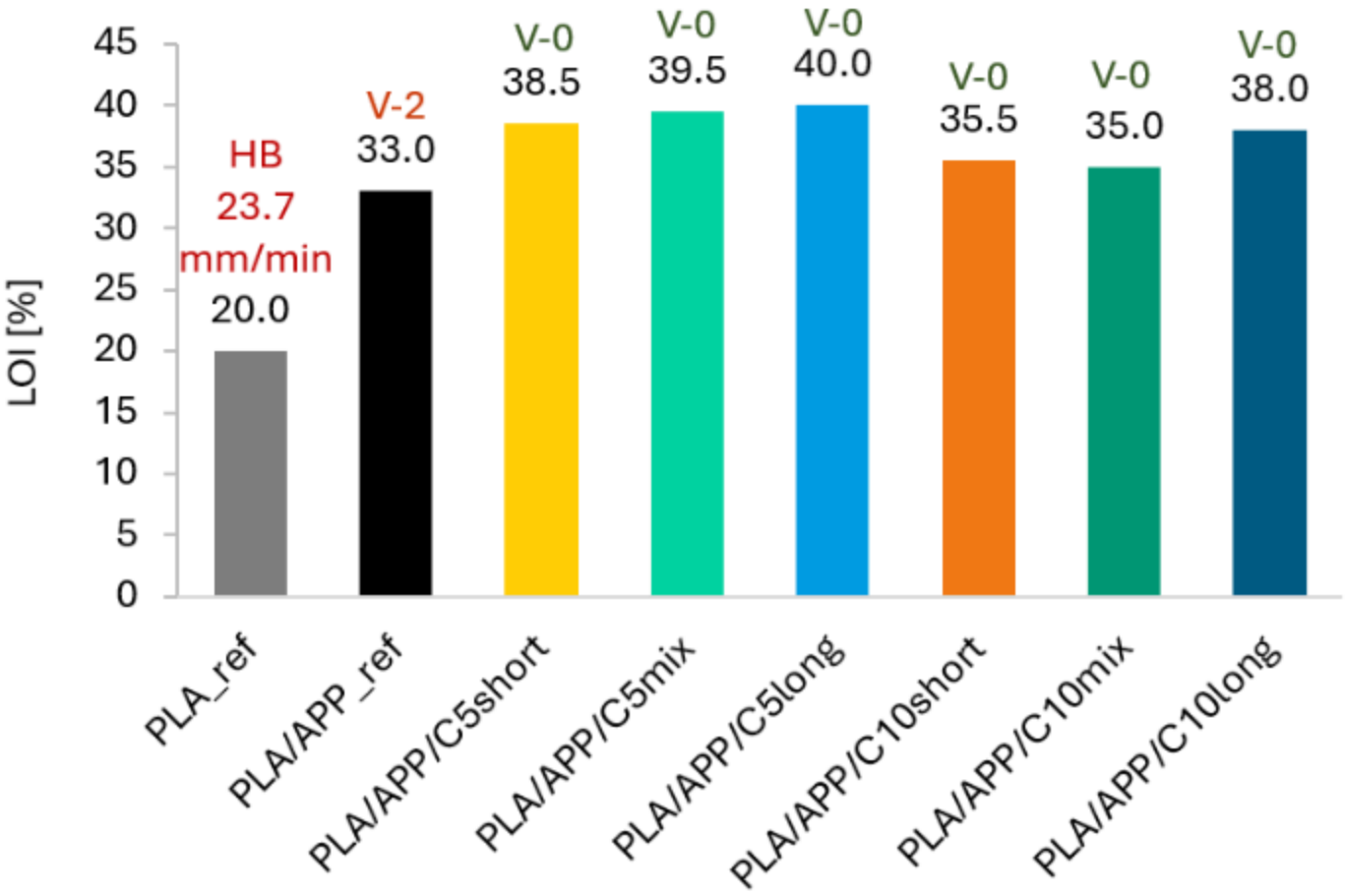


Figure 1

LOI and UL 94 rating of PLA/APP/cellulose composites

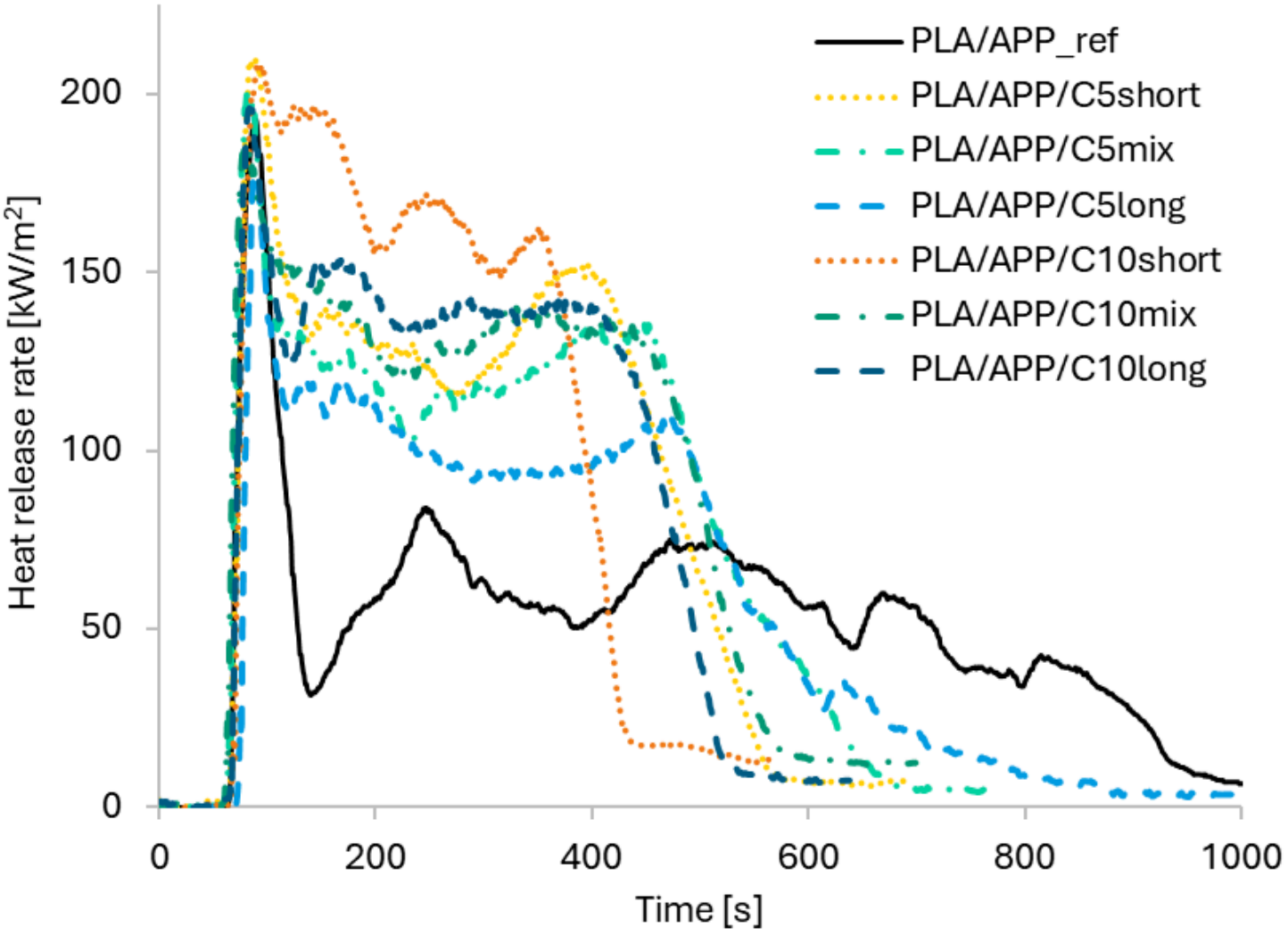


Figure 2

Heat release rate curves of PLA/APP/cellulose composites

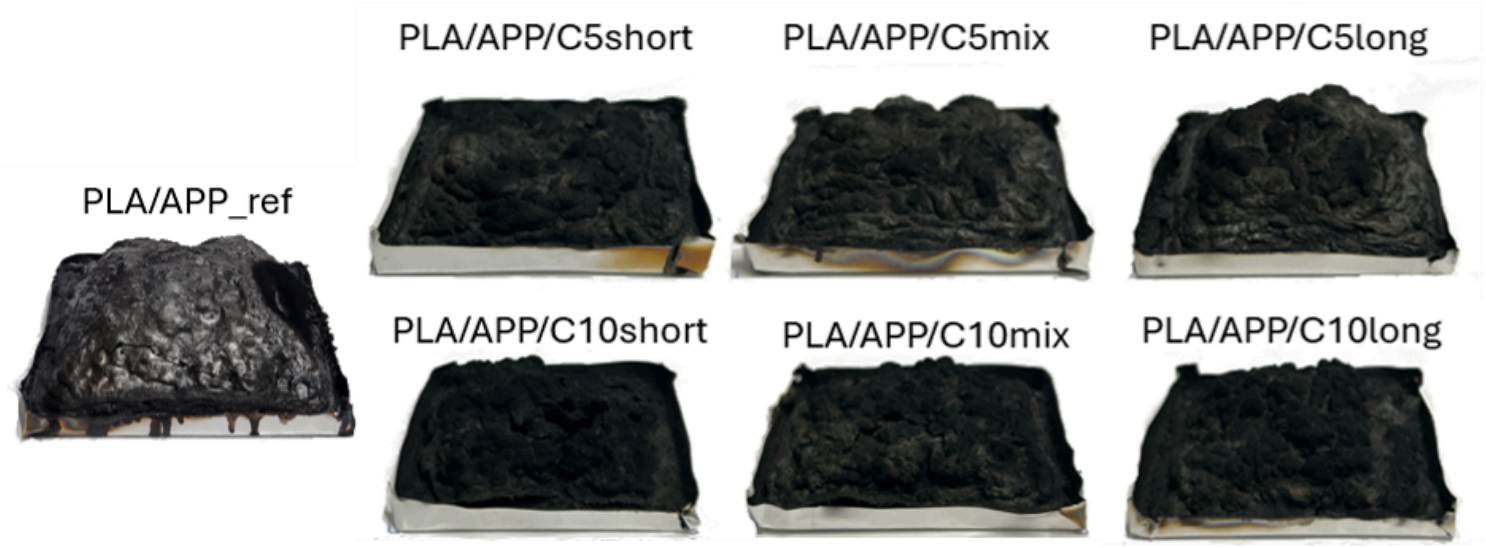


Figure 3

Combustion residues obtained after cone calorimeter tests

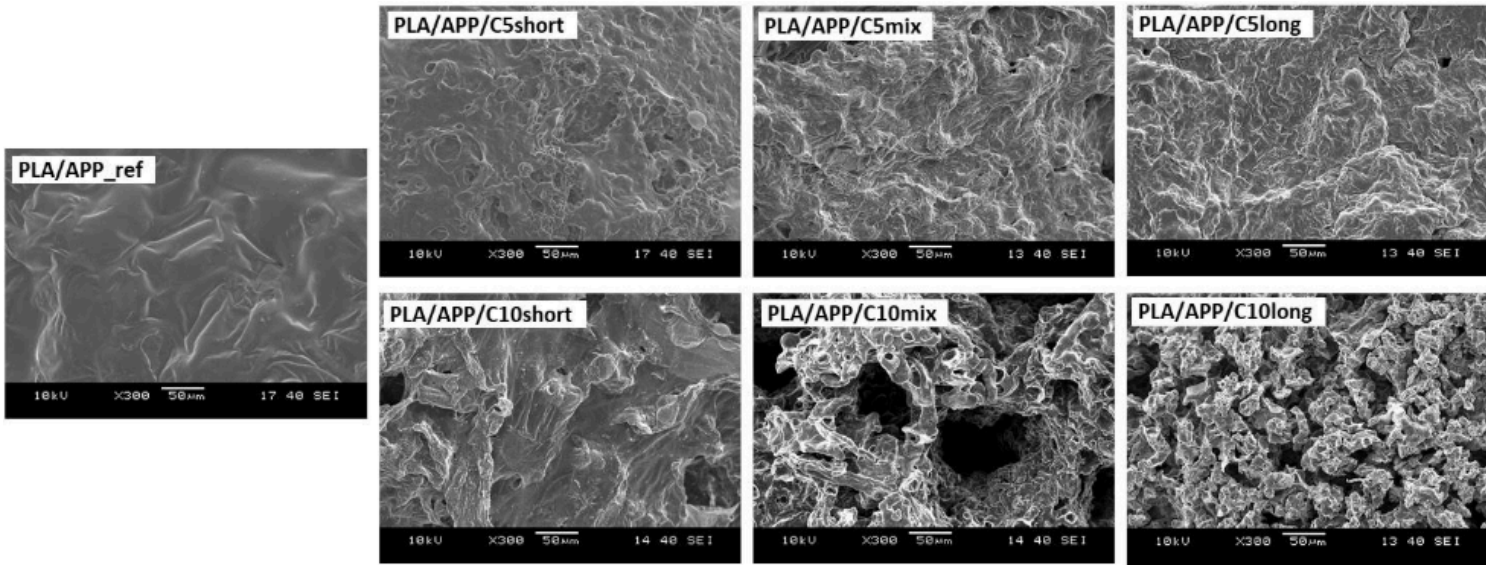


Figure 4

SEM micrographs taken of the combustion residues obtained after cone calorimeter tests

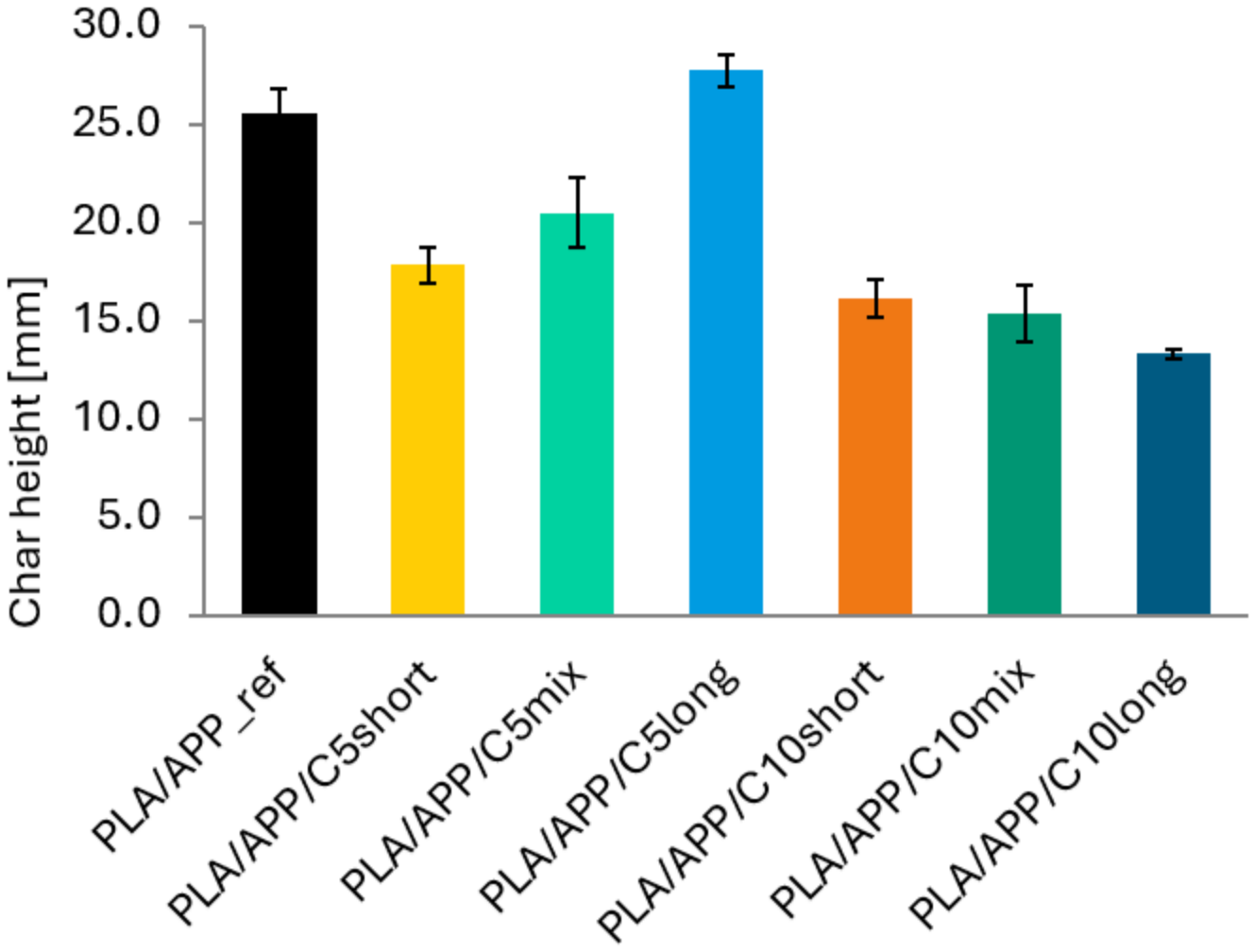


Figure 5

Height of the char residue formed after combustion under a cone heater at a constant heat flux of 35 kW/m^2 for 5 min.

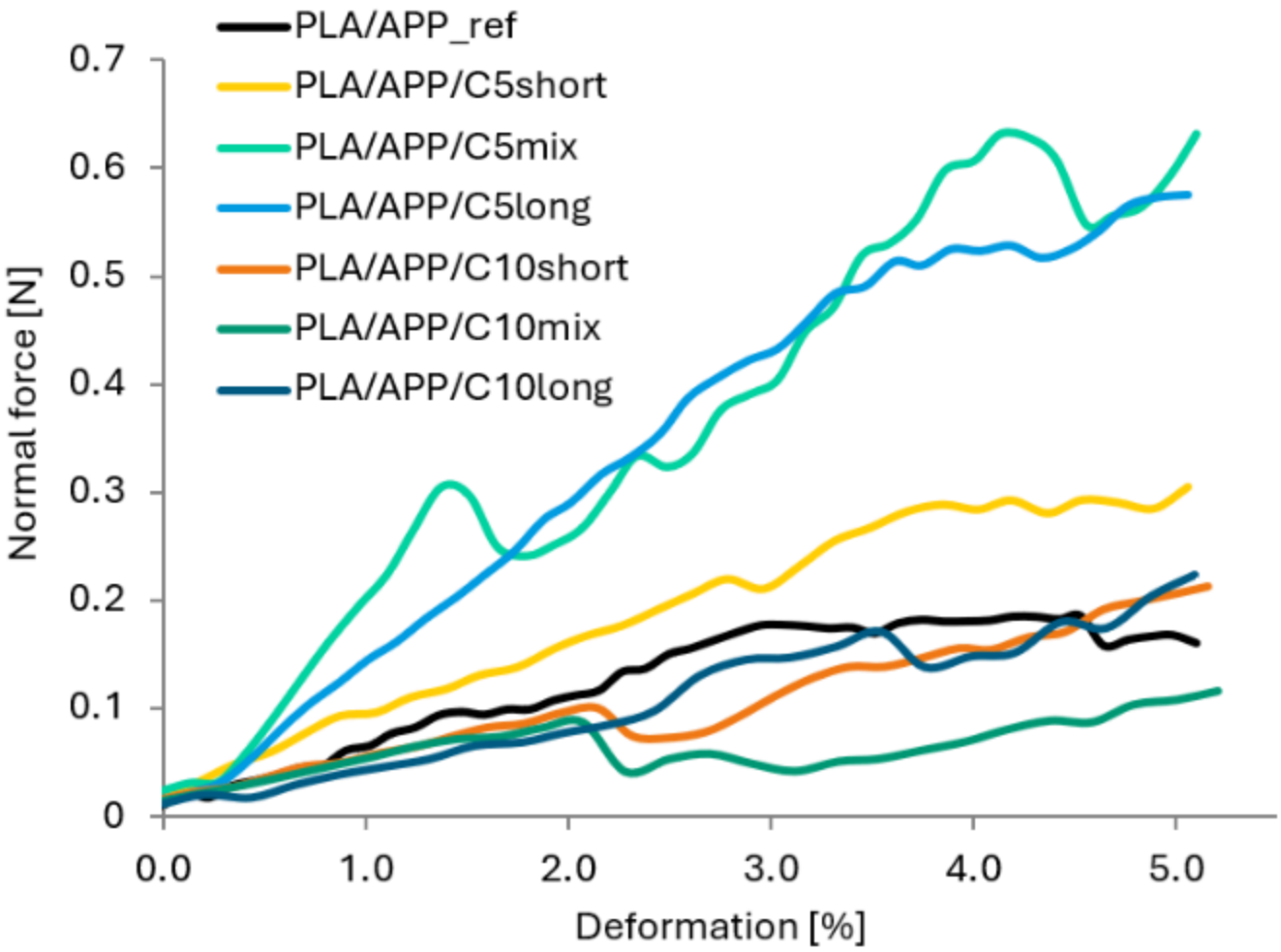


Figure 6

Compression force–deformation curves of the combustion residues (chars) of PLA/APP/cellulose composites.

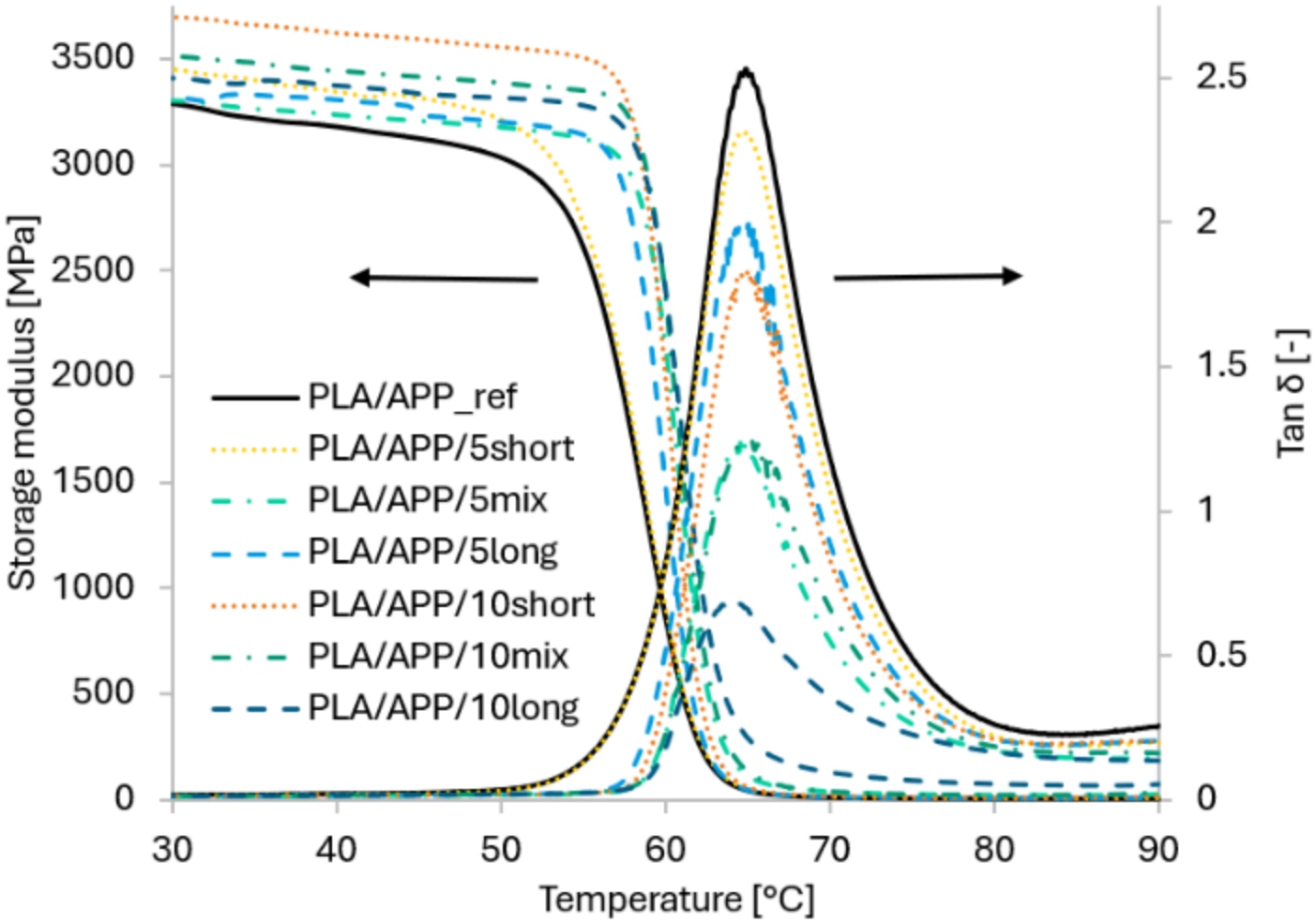


Figure 7

DMA results of of PLA/APP/cellulose composites

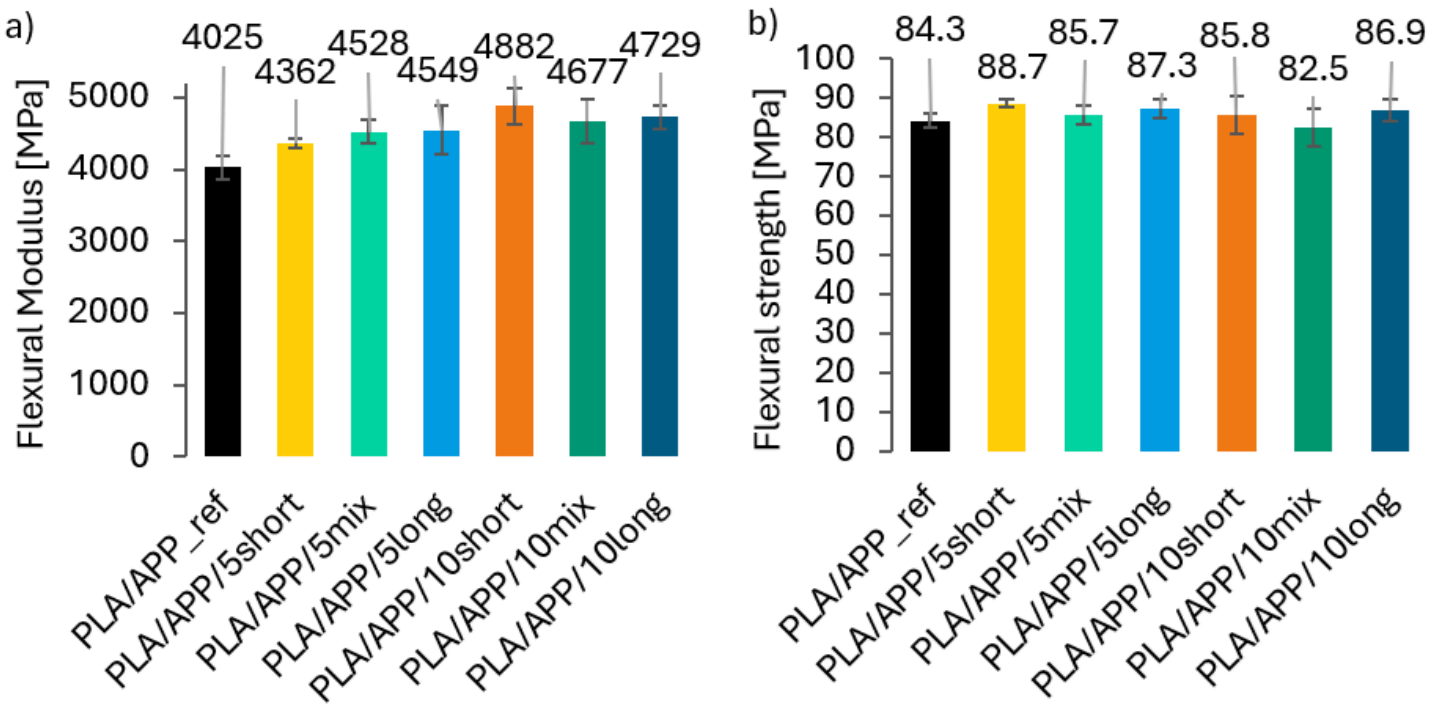


Figure 8

Three-point bending test results of PLA/APP/cellulose composites

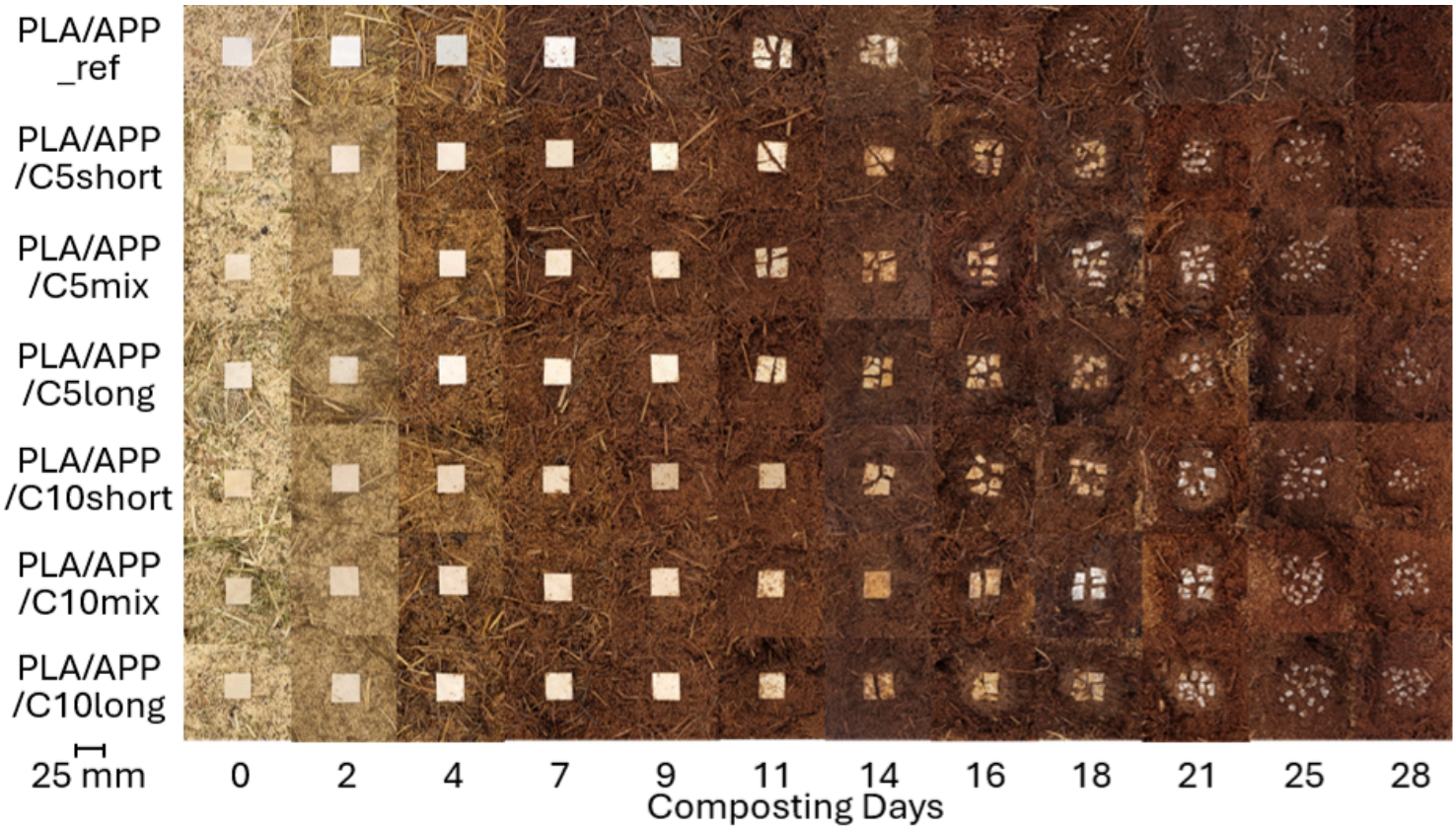


Figure 9

Photos of the composted samples over time